

Filter-bank design for multicarrier modulation systems with MPSK based on symbol-error-rate evaluation

Y. Wang and X.-P. Zhang

Abstract: A novel complex-valued filter-bank design method, for generic multicarrier-modulation (MCM) systems with M -ary phase-shift keying (MPSK), is presented to minimise the symbol error rate (SER). The SER is evaluated by a newly derived closed-form formula, which can be used to evaluate both discrete-Fourier-transform (DFT)-based orthogonal-frequency-division-multiplexing (OFDM) and discrete-wavelet-multitone (DWMT) systems. Monte-Carlo numerical simulations are performed to verify the theoretical SER analysis and compare the error performance of the proposed MCM system with DFT-based OFDM and DWMT systems. It is shown that the derived formula is consistent with simulation results and the newly designed complex-valued filter-bank-based MCM system outperforms conventional DWMT systems in terms of the SER and has comparable SER performance with DFT-based OFDM systems with cyclic prefix (CP).

1 Introduction

In recent years, multicarrier modulation (MCM) has become increasingly popular as a transmission technique, especially in high-speed communications, including wireline and wireless systems. The principle of MCM consists of splitting up a wideband signal at a high symbol rate into several lower rate signals, each occupying a narrower band which is called a subchannel or a subcarrier. By dividing the input data stream into parallel substreams and each stream being modulated on one of a set of subchannels at different carrier frequencies, the power spectrum of the transmitted signal can be shaped to match the channel characteristics and achieve near-optimal performance in theory. Hence, a generally recognised advantage of MCM is its robustness against various types of channel distortions, such as multipath propagation and narrowband interference [1, 2]. MCM systems have been under intensive research and development in recent years, and M -ary phase-shift keying (MPSK) has been adopted as an important modulation scheme for MCM systems [3–5]. In MCM modulation, subcarriers are made mutually orthogonal, so that the receiver can separate these subcarriers even if there is spectral overlapping among them. Figure 1 shows the block diagram for an MCM transceiver. The transmitter accepts a serial data stream and converts it into several low rate parallel sequences of subchannel symbols (S/P). Symbols of each subchannel are coded with various coding schemes and then modulated on a subcarrier with a filter-bank-based modulator. The output of the modulator, a single composite signal sequence, is modulated on a radio-frequency (RF) carrier and transmitted through a channel. At the receiver

end, after RF demodulation, the multicarrier demodulation is accomplished with a filter-bank demodulator. After decisions are made for all subchannel symbols, the decoded data sequences are then converted back to a single serial data stream (P/S). The filter-bank-based modulator and demodulator of a generic MCM system are illustrated in Fig. 2.

Mainly two types of filter banks are adopted as modulators and demodulators in generic MCM systems. The first one, also known as orthogonal frequency division multiplexing (OFDM), is based on discrete-Fourier-transform (DFT) filter banks. The OFDM was proposed decades ago [6] and has found broad applications such as European digital audio broadcasting (DAB), European digital video broadcasting (DVB), short-range wireless access and wireless LAN standards (IEEE802.11a). The

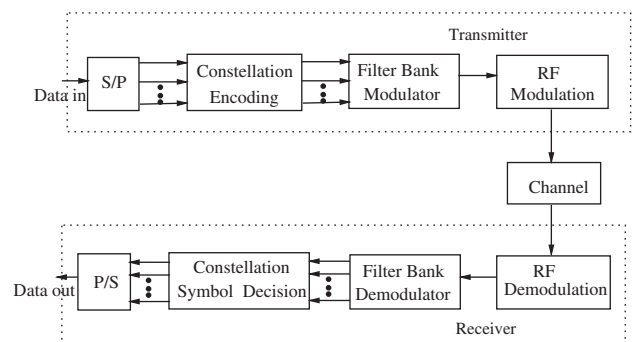


Fig. 1 Block diagram for a generic MCM transceiver

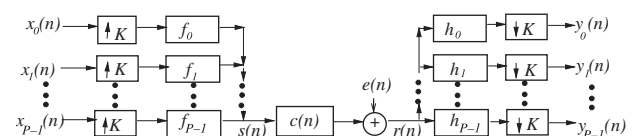


Fig. 2 Block diagram for filter-bank-based modulator and demodulator in generic MCM systems

© The Institution of Engineering and Technology 2006

IEE Proceedings online no. 20050133

doi:10.1049/ip-com:20050133

Paper first received 30th March 2005 and in final revised form 6th February 2006

The authors are with the Department of Electrical and Computer Engineering, Ryerson University, 350 Victoria Street, Toronto, Ontario, M5B 2K3, Canada
E-mail: xzhang@ee.ryerson.ca

DFT filter bank exhibits the desired mutual orthogonality of subchannels and can be implemented by a fast Fourier transform (FFT). The other type of filter banks, which is generated from a well-designed prototype filter via extended lapped transform (ELT), has been proposed for discrete wavelet multitone (DWTMT) systems as another realisation of MCM [1, 7–9]. Adopted as one of the signaling standards for asymmetric digital subscriber lines (ADSL), a DWTMT system can achieve a high level of subchannel spectral containment, so that it is more robust with regard to interchannel interference and narrow-band channel noise compared to DFT-based OFDM [1].

In most practical MCM systems, the mutual orthogonality of subchannels is often destroyed by nonideal channels, therefore the transmitted symbols for a given subchannel may be distorted by co-subchannel symbols (intersymbol interference or ISI) and symbols of other subchannels (interchannel interference or ICI), as well as channel noise. For DFT-based OFDM, the high degree of the spectral overlapping among subchannels of DFT filter banks makes it difficult to retain subchannel isolation for multipath channels, therefore a technique in which a cyclic prefix (CP) is inserted at the beginning of each data segment has been adopted at the cost of system efficiency [10, 11], to partially offset the interference introduced by channels. Owing to the existence of ISI, ICI and channel noise in an MCM system, an expression of the symbol error rate (SER), which is one of the essential parameters for system performance evaluations, cannot be obtained readily. Some attempts based on certain assumptions and bounds have been made to analyse the error performance of DFT-based OFDM systems [5, 12–17]. However, the error performance of a generic MCM system, where the modulation filters form a set of orthonormal basis, such as a DWTMT system, has not been systematically investigated.

In this paper, the error performance of a generic MCM system, with DFT-based OFDM and DWTMT as two realisations, is studied by considering the effects of two types of interferences and additive channel Gaussian noise. By studying the constellations of received symbols and interferences for a given subchannel, and by modelling the sum of ISI and ICI as a Gaussian process using the central limit theorem (CLT), the error performance of a given subchannel in a generic MCM system is analysed in the presence of additive Gaussian noise. Furthermore, by adopting the conventional optimal phase detector in each subchannel, we derive a closed-form expression for the SER for a generic MCM system employing MPSK. This SER formula is verified with numerical Monte-Carlo simulations for DFT-based OFDM systems and conventional discrete wavelet multitone (DWTMT) systems.

By using the derived SER formula as an objective function, a novel MCM system based on complex-valued unitary filter banks is presented with improved error performance. Unlike real-valued coefficient filters, complex-valued filters have asymmetric frequency responses and are more suitable to deal with complex-valued signals which are often present in communication systems. The unitary filter bank is a good candidate for an MCM modulator/demodulator due to the inherent mutual orthogonality between filters. Filters in the presented MCM are parameterised with free parameters, which can be adjusted to different applications. By taking the SER as the objective function, the free parameters can be optimised based on the error performance. Simulation results show that the new MCM system based on designed filter banks outperforms the DWTMT system in terms of the SER, and its SER performance is comparable to that of the DFT-based

OFDM system with CP, which is less efficient in terms of the transmission rate.

Boldface lower-case letters are used to represent vectors and boldface upper-case letters are reserved for matrices. The notations \mathbf{A}^T and \mathbf{A}^H represent the transpose and transpose conjugate of \mathbf{A} . The superscript $*$, as in \mathbf{A}^* , denotes the conjugation only. The Kronecker delta function $\delta(n)$ is defined as

$$\delta(n) = \begin{cases} 1, & n = 0 \\ 0, & n \neq 0 \end{cases} \quad (1)$$

2 SER evaluation for MCM systems with MPSK modulation

2.1 System modelling

The filter-bank-based modulator and demodulator, with P subchannels, of a generic MCM system are illustrated in Fig. 2. The modulation and demodulation filters of subchannel p , $0 \leq p \leq P-1$, are denoted, respectively, as f_p and h_p , which are of length $L = gK$, where g is the overlapping factor which is a positive integer. Upsampling/downsampling factor is denoted as K . Assume the transmission channel has finite impulse response (FIR) with channel length L_c , denoted by $c(n)$, $n = 0, \dots, L_c - 1$.

The modulation filters f_p , $0 \leq p \leq P-1$, should fulfil the orthogonality property [1], i.e. for $0 \leq p_1, p_2 \leq P-1$,

$$\sum_{l=0}^{L-1} f_{p_1}(l) f_{p_2}^*(l - nK) = \delta(n) \delta(p_1 - p_2) \quad (2)$$

Moreover, the modulation and demodulation filters satisfy the perfect reconstruction (PR) property defined as in [18]

$$\sum_{l=0}^{L-1} f_{p_1}(l) h_{p_2}(nK - l) = \delta(n) \delta(p_1 - p_2) \quad (3)$$

Both DFT-based OFDM and DWTMT systems are special cases of generic MCM systems. For DFT-based OFDM, the lowpass modulation filter is chosen as

$$f_0(l) = \begin{cases} \frac{1}{\sqrt{P}}, & 0 \leq l \leq L-1 \\ 0, & \text{otherwise} \end{cases} \quad (4)$$

Then, the other $P-1$ modulation filters are obtained by rotating the low pass filter to

$$f_p(l) = f_0(l) e^{j\omega_p l} \quad (5)$$

where $\omega_p = 2\pi p/P$, $p = 1, \dots, P-1$. The inclusion of zero-padded CP can be implemented by choosing the upsampling/downsampling factor $K = P + L_k$, where L_k is the length of the CP and it is no shorter than the length of the transmission channel $c(n)$. Demodulation filters are generated as follows to remove the CP that is added at the transmitted end:

$$h_p(l) = \begin{cases} 0 & -P - L_k + 1 \leq l \leq -P \\ f_p^*(-l) & -P + 1 \leq l \leq 0 \end{cases} \quad (6)$$

For DFT-based OFDM, the overlapping factor $g = 1$. The length of filters for a DFT-based OFDM system with CP is $L = P + L_k$.

For a conventional real-valued cosine-modulated filter-bank-based DWTMT system, $K = P$ and modulation filters are generated as [8]:

$$f_p(l) = w(l) \sqrt{\frac{2}{P}} \cos\left(\left(p + \frac{1}{2}\right)\left(l + \frac{P+1}{2}\right)\frac{\pi}{P}\right) \quad (7)$$

for $p = 0, 1, \dots, P-1$, where $w(l)$ is the impulse response of a lowpass filter with length $L = gP$ and $g \geq 2$. The demodulation filters of a DWT system can be obtained by

$$h_p(l) = f_p(-l), 0 \leq l \leq L-1 \quad (8)$$

The transmission channel $c(n)$ is modelled as a linear-time-invariant (LTI) FIR (finite-impulse-response) filter of length L_c , followed by a stationary zero-mean Gaussian noise source $e(n)$, which is independent of transmitted symbols $\{x_p(n), p = 0, 1, \dots, P-1\}$. Note that $c(n)$ can be considered as the overall transfer function resulting from the real communication channel and a time-domain equaliser (TEQ), which precedes the filter-bank demodulator in cases where a TEQ is employed.

For an MCM system with the MPSK modulation scheme, abbreviated as an MPSK-MCM system, a conventional optimal-phase detector is employed for each subchannel to calculate the phase of each received symbol and decode the received symbol with preset phase boundaries. The SER for a generic MPSK-MCM system is derived in the following Subsection.

2.2 SER for generic MPSK-MCM systems

In MCM systems, at each time frame n_1 , P parallel symbols $\{x_0(n_1), x_1(n_1), \dots, x_{P-1}(n_1)\}$ are transmitted, with each symbol modulated to one of the P subchannels. The transmitted subchannel symbol in subchannel p_1 at frame n_1 , $x_{p_1}(n_1)$, represents constellation points generated by a modulation scheme such as MPSK. Corresponding to each transmitted constellation point, $x_{p_1}(n_1)$, there is a received symbol $y_{p_1}(n_1 + d)$, where d is the system delay. If only the delay involved in the convolution with the modulation and demodulation filters, both of length $L = gK$, is considered, then $d = g$. The following formulation gives the expression of $y_{p_1}(n_1 + d)$.

Formulation 1: In an MCM system shown in Fig. 2, assume the channel impulse response is $c(n)$, $n = 0, 1, \dots, L_c - 1$, and the zero-mean additive Gaussian noise is $e(n)$. Then, for a given subchannel p_1 , the received symbol $y_{p_1}(n_1 + d)$, corresponding to the symbol $x_{p_1}(n_1)$ transmitted at time frame n_1 , can be expressed as

$$y_{p_1}(n_1 + d) = \bar{y}_{p_1} + \xi + \zeta \quad (9)$$

where \bar{y}_{p_1} is the contribution from symbol $x_{p_1}(n_1)$, ξ is the contribution from channel noise and ζ is the interference item calculated by summing up all ICI and ISI items. Note that $x_{p_1}(n_1)$ is the only transmitted symbol contributing to \bar{y}_{p_1} , which can be expressed as follows:

$$\bar{y}_{p_1} = \alpha_{p_1 p_1}(n_1) x_{p_1}(n_1) \quad (10)$$

ξ can be calculated as

$$\xi = \sum_{n=-\infty}^{\infty} e(n) h_{p_1}(n_1 K - n) \quad (11)$$

and ζ can be calculated as

$$\begin{aligned} \zeta = & \sum_{n=-\infty}^{\infty} \sum_{p \neq p_1, p=0}^{P-1} \alpha_{p p_1}(n) x_p(n) \\ & + \sum_{n \neq n_1, n=-\infty}^{\infty} \alpha_{p_1 p_1}(n) x_{p_1}(n) \end{aligned} \quad (12)$$

In (10) and (12), $\alpha_{p p_1}(n)$, for $0 \leq p, p_1 \leq P-1$, is the weight of the contribution from the transmitted symbol

$x_p(n)$ to the received symbol $y_{p_1}(n_1 + d)$, and is calculated as

$$\alpha_{p p_1}(n) = \sum_{j=0}^{L_c-1} c(j) \sum_{l=0}^{L-1} f_p(l) h_{p_1}[(n_1 - n)K - j - l] \quad (13)$$

where L_c is the length of channel impulse response $c(n)$. (For the derivation of Formulation 1, see the Appendix, Section 7.1.)

Remarks: When the filter-bank-based modulator/demodulator and the communication channel are all LTI, the term \bar{y}_{p_1} in (9) is deterministic for a given transmitted symbol $x_{p_1}(n_1)$. According to (10), \bar{y}_{p_1} is a weighted version of $x_{p_1}(n_1)$ and the weight $\alpha_{p_1 p_1}(n_1)$ is a constant for a given subchannel p_1 . Hence, in general, the constellation points of $x_{p_1}(n_1)$ and \bar{y}_{p_1} are a one-to-one mapping. For each constellation point of $x_{p_1}(n_1)$, as defined in (37), there is a corresponding constellation point \bar{y}_{p_1} which can be calculated by (10). All the possible values of \bar{y}_{p_1} form the set of constellation points at the receiving end of subchannel p_1 . Both noise item ξ and interference item ζ are random processes.

A new closed-form SER formula for generic MPSK-MCM systems is then given in the following theorem.

Theorem 1: When the transmitted symbols $x_p(n)$, $0 \leq p \leq P-1$, are coded by the MPSK scheme with symbol energy ϵ_x , and the optimal phase detector for each subchannel is adopted at the receiver end, the SER of the received symbol $y_{p_1}(n_1 + d)$ at subchannel p_1 , which corresponds to the transmitted symbol $x_{p_1}(n_1)$, can be determined as

$$P_{e, p_1} = \frac{1}{\pi} \int_0^{\frac{(M-1)\pi}{M}} \exp\left(-\frac{\gamma \sin^2(\pi/M)}{2 \sin^2(\phi)}\right) d\phi \quad (14)$$

where

$$\gamma = \frac{|\alpha_{p_1 p_1}(n_1)|^2 \epsilon_x}{\left[\sum_{p, p \neq p_1} \sum_n |\alpha_{p p_1}(n)|^2 + \sum_{n, n \neq n_1} |\alpha_{p_1 p_1}(n)|^2 \right] \epsilon_x + \sigma_n^2} \quad (15)$$

is the signal-to-noise- and -interference ratio (SNIR), σ_n^2 is the variance of zero mean additive Gaussian noise $e(n)$ and $\alpha_{p p_1}(i)$ is defined in (13). See Appendix, Section 7.2 for proof of Theorem 1.

The overall SER for the MCM system, P_e , can be obtained by averaging P_{e, p_1} over all subchannels,

$$P_e = \frac{1}{P} \sum_{p_1=0}^{P-1} P_{e, p_1} \quad (16)$$

2.3 SER expression for AWGN channels

For an AWGN channel or a channel that has been perfectly equalised, the expression of the SER for a generic MCM system is trivial and can be simplified on the basis of (15). For an AWGN channel, $c(n) = \delta(n)$. It can be seen from (3) that

$$\alpha_{p p_1}(n) = \delta(p - p_1) \delta(n - n_1) \quad (17)$$

i.e. the only symbol which has nonzero contribution to $y_{p_1}(n_1 + d)$ is $x_{p_1}(n_1)$. As $\sigma_y^2 = \sigma_n^2$, the SNIR γ in (15)

becomes

$$\gamma = \rho = \frac{\epsilon_x}{\sigma_n^2} \quad (18)$$

which is the signal-to-noise ratio (SNR). From (16), the overall SER, P_e , is

$$P_e = P_{e,p_1} \quad (19)$$

By substituting (17) into (14), we obtain the SER for an MPSK-MCM system, which is identical to the SER formula for a single-carrier MPSK system over AWGN channels. With the increase of SNR, the SER will decrease quickly. It can also be seen from (19) that, for an AWGN channel, the number of subchannels, P , has no effect on the system error performance. Figure 3 shows the SER results for both single-carrier modulation and the conventional DWMT modulation, with different numbers of subchannels, over an AWGN channel. The coding scheme adopted is binary phase-shift keying (BPSK).

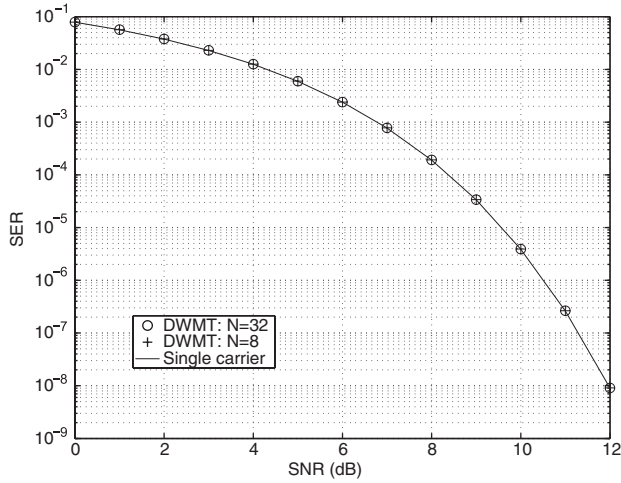


Fig. 3 Error performance of single carrier modulation and conventional DWMT ($g=2$) modulation with BPSK

2.4 SER expression for frequency selective channels

To investigate the performance of MCM systems over generic frequency selective channels, we rewrite γ in (15) in an alternative expression as

$$\gamma = \frac{|\alpha_{p_1 p_1}(n_1)|^2 \rho}{\left[\sum_{p, p \neq p_1} \sum_n |\alpha_{pp_1}(n)|^2 + \sum_{n, n \neq n_1} |\alpha_{p_1 p_1}(n)|^2 \right] \rho + 1} \quad (20)$$

It can be seen from (20) that, when the SNR ρ is much larger than 1(0dB) and interferences (ICI and ISI) are not negligible, P_{e,p_1} is dominated by the ratio of weights for desired symbol and interferences, which can be approximated as

$$\gamma \approx \frac{|\alpha_{p_1 p_1}(n_1)|^2}{\sum_{p, p \neq p_1} \sum_n |\alpha_{pp_1}(n)|^2 + \sum_{n, n \neq n_1} |\alpha_{p_1 p_1}(n)|^2} \quad (21)$$

In this case, the SER performance will not change much with the increase of SNR ρ . Figure 4 shows the error performance of a DWMT system, with overlapping factor $g=2$, over a sample frequency-selective channel.

For DFT-based OFDM systems, from (13), the inclusion of zero-padded CP does not change the value of numerator in (21), but the values of denominator will decrease because of the increase of the upsampling/downsampling factor K .

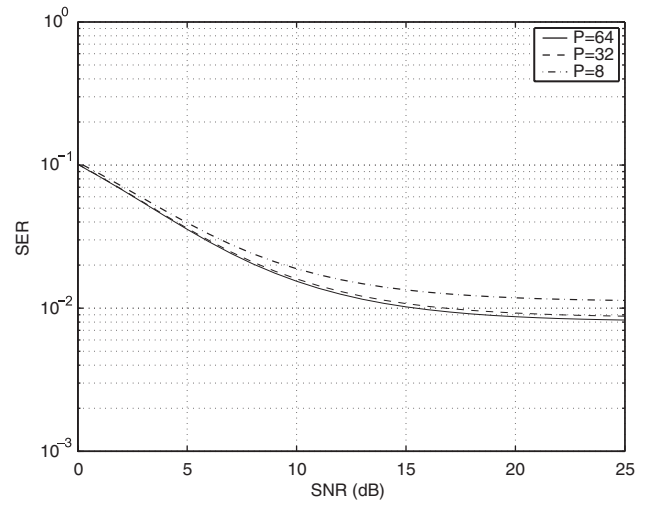


Fig. 4 Error performance of conventional DWMT systems ($g=2$) over channel $c(n) = [1, 0.5e^{j\pi/6}, 0.3e^{-j\pi/3}, 0.2e^{j\pi/2}, 0.1]$

Hence, CP included in OFDM systems will demonstrate superior error performance to MCM systems without CP.

Note that, here, the frequency-selective channel is assumed to be stationary and time-invariant, such as in wireline applications including DSL, or slow-fading wireless multipath channels over the observation period. It is an interesting future research topic to further investigate the SER expressions of MCM systems for wireless channels with both time-varying fading, such as in [17, 19, 20] and frequency-selective fading.

Expressions of (14) and (16) provide a systematic approach to calculate the SER of a generic MCM system, whose filter banks fulfil the orthogonality and PR conditions in (2) and (3). Moreover, the SER formulas can be used as objective functions in the design of modulation and demodulation filter banks for an MCM system to achieve better error performance. In the following, a novel MCM system is presented based on complex-valued unitary filter banks designed to minimise the SER.

3 Complex-valued unitary filter-banks-based MCM system design

Unitary filter banks are a special class of maximally decimated ($P=K$) PR filter banks. A unitary filter bank is a good candidate to the modulator/demodulator for an MCM system, because of the inherent mutual orthogonality among its filters. Unitary filter banks with FIR filters have many useful properties. Among these properties are that they can be completely factorised, are easy to implement with a lattice structure and have no questions of stability [18]. Moreover, they can be used to construct orthonormal multiband wavelet bases, which are powerful tools for nonstationary signal analysis. Owing to the existence of complex-valued signals in wireless systems, complex-valued filters, which have asymmetric frequency responses, are employed in this paper. The complex-valued filter bank is completely parameterised and the coefficients of all filters are expressed with free parameters, which can be determined depending on different applications. In this paper, the SER expressed in (14) and (16) of an MCM system which employs an MPSK modulation scheme for all P subchannels, is used as the objective function to optimise the performance of the presented novel MCM system based on the complex-valued filter bank.

3.1 Parameterisation of filter-bank coefficients

The Householder factorisation of polyphase component matrices of modulation filters $\{f_0, f_1, \dots, f_{P-1}\}$ for complex-valued unitary filter banks can be summarised as follows [18, 21]. The z -transform of filter $f_p, p = 0, 1, \dots, P-1$ can be formulated in a polyphase form as

$$\mathbf{F}_p(z) = \sum_{k=0}^{P-1} z^{-k} \mathbf{F}_{p,k}(z^P) \quad (22)$$

Define the polyphase component matrices as follows:

$$(\mathbf{F}(z))_{p,k} = \mathbf{F}_{p,k}(z) \quad (23)$$

If $\mathbf{F}(z)$ is a unitary matrix, i.e.

$$\mathbf{F}^T(z^{-1})\mathbf{F}(z) = \mathbf{I} \quad (24)$$

where \mathbf{I} is the identity matrix, then $\mathbf{F}(z)$ has the Householder factorisation

$$\mathbf{F}(z) = \left\{ \prod_{n=1}^{J-1} [\mathbf{I} - \mathbf{v}_n \mathbf{v}_n^H + z^{-1} \mathbf{v}_n \mathbf{v}_n^H] \right\} \mathbf{V} \quad (25)$$

where J is the McMillan degree of $\mathbf{F}(z)$, \mathbf{v}_n is the unit-norm Householder parameters and \mathbf{V} is a $P \times P$ constant unitary matrix and can be selected according to various applications. As a special case, for filter banks associated with P -band wavelet transform, the unitary matrix \mathbf{V} may be generated by assigning one column as a constant vector $\left[\frac{1}{\sqrt{P}}, \frac{1}{\sqrt{P}}, \dots, \frac{1}{\sqrt{P}} \right]^T$, which corresponds to the scaling filter, and then adding orthogonal columns to generate wavelet filter vectors [22, 23]. The $P-1$ orthogonal columns may be produced via the Gram-Schmidt process in $\binom{P-1}{2}$ ways.

The Householder parameters are of unit norm, therefore each Householder parameter in (25) can be further parameterised as [21]

$$\mathbf{v}_{n,j} = \begin{cases} \left[\prod_{k=0}^{j-1} \sin(\theta_{n,k}) \right] \cos(\theta_{n,j}) e^{j\phi_{n,j}}, & j = 0, 1, \dots, P-2 \\ \prod_{k=0}^{P-2} \sin(\theta_{n,k}), & j = P-1 \end{cases} \quad (26)$$

for $n = 1, \dots, J-1$, i.e. $\mathbf{v}_{n,j}$ can be determined by $2(P-1)$ angle parameters. After \mathbf{V} is determined, filter bank $\{h_0, h_1, \dots, h_{P-1}\}$ can be determined by $2(J-1)(P-1)$ angle parameters. The length of filters $f_p, p = 0, 1, \dots, P-1$, is $L = JP$.

The relation between modulation filters and demodulation filters can be expressed as

$$h_p(l) = f_p^*(-l) \quad (27)$$

where $p = 0, 1, \dots, P-1$ and $l = 0, 1, \dots, L-1$.

3.2 SER improvement based on proposed filter banks

To calculate all filter coefficients in (25), constant matrix \mathbf{V} and free parameters $\theta_{n,k}, \phi_{n,j}$, in (26), should all be determined. The procedure to design a novel MCM system based on the P -band unitary filter bank to optimise the SER performance is outlined as follows:

- *Step 1:* Choose the unitary matrix \mathbf{V} according to different applications. For simplicity, we propose \mathbf{V} as the $P \times P$

DFT matrix, which is defined as

$$\mathbf{V}_{nk} = \sqrt{\frac{1}{P-1}} e^{-j2\pi(k-1)(n-1)} \quad (28)$$

for $k, n = 1, 2, \dots, P$.

- *Step 2:* Define the objective function. We take the average SER formula for an MPSK coded MCM system expressed in (16) and (14) as the objective function:

$$P_e = \frac{1}{P} \sum_{p_1=0}^{P-1} P_{e,p_1} \quad (29)$$

where P_{e,p_1} can be calculated by

$$P_{e,p_1} = \frac{1}{\pi} \int_{\frac{(M-1)\pi}{M}}^{\pi} \exp\left(\frac{\gamma \sin^2(\pi/M)}{2 \sin^2(\phi)}\right) d\phi \quad (30)$$

where γ is a function of coefficients of modulation/demodulation filters, which in turn are functions of free parameters $\theta_{n,j}$ and $\phi_{n,j}$, $j = 0, 1, \dots, P-2$, $n = 0, 1, \dots, J-1$.

- *Step 3:* Apply a numerical optimisation method to determine the values of free parameters. First, set up initial values for all free parameters $\theta_{n,j}$ and $\phi_{n,j}$, $j = 0, 1, \dots, P-2$, $n = 0, 1, \dots, J-1$, then a conjugate gradient method can be used to minimise the $2(J-1)(P-1)$ dimensional function P_e . Note that the optimisation may fall into a local minimum, which is common for a nonlinear objective function. Some global optimisation methods such as adding random interference and simulated annealing may also be used. However, in practice, a local minimum may be satisfactory, if it attains desirable SER requirements.

4 Simulations

To verify our theoretical analysis of error performance of a generic MCM system, Monte-Carlo numerical simulations are performed with three types of MCM systems, namely, the DFT-based OFDM system with zero-padded CP which is no shorter than the length of the channel, the DFT-based MCM without cyclic prefix and the conventional DWMT systems with overlapping factor $g = 2$. The modulation filters for the conventional DWMT systems are generated by a prototype filter [24]

$$w(l) = \sin\left(\frac{\pi}{2P} \left(l + \frac{1}{2}\right)\right) \quad (31)$$

for $l = 0, 1, \dots, P-1$. Both the AWGN channel and frequency-selective channels are considered in the simulations.

Transmitted data streams $x_p(n)$, $p = 0, 1, \dots, P-1$, are generated according to (37). The composite data sequence before entering the channel, $s(n)$, as illustrated in Fig. 2, is obtained by first upsampling each of the MPSK symbol streams $\{x_0(n), x_1(n), \dots, x_{P-1}(n)\}$ by factor K , then convolving each data stream with one of the P subchannel modulation filters, finally summing up the outputs of all P modulation filters. After convolution of one $s(n)$ with the channel $c(n)$, AWGN noise, for which power is simulated according to a particular SNR, is added to the transmitted sequence to obtain distorted data sequence $r(n)$. Then $r(n)$ is passed through the demodulation filter of each subchannel, and the resulting signals are downsampled by factor K . The optimal phase detector is employed for each subchannel according to the phase detection boundary

in (44). Matching of the detected symbol with the original data is made and errors are counted to obtain the SER for a particular SNR.

Figure 5 shows both analytical and simulation results over an AWGN channel for DFT-based OFDM systems, with and without zero-padded CP, and DWMT with $g = 2$. The modulation scheme is quadrature-phase-shift keying (QPSK). It can be seen that our theoretical analysis matches the simulations results. In addition, all three kinds of MCM systems exhibit the same error performance as that in single-carrier systems over an AWGN channel. The identical SER performance of single-carrier systems and MCM systems over the AWGN channel has been explained in Section 2.3.

Figures 6 and 7 show the results of these MCM systems, with $P=32$ subchannels, over two sample frequency-selective channels with impulse response $c_1(n)=[1, 0.5e^{j\pi/6}]$ and $c_2(n)=[1, 0.5e^{j\pi/6}, 0.3e^{-j\pi/3}, 0.2e^{j\pi/2}, 0.2, 0.1]$, for QPSK symbols. Each simulation result demonstrates the consistency with corresponding theoretical analysis. As expected, the DFT-based OFDM system with CP has superior SER over the other two MCM systems, with the cost of system transmission efficiency. It is also demonstrated that the DWMT has the poorest SER. The reason is that both channels have no narrow-band interference in comparison to the bandwidth of the subchannels, therefore

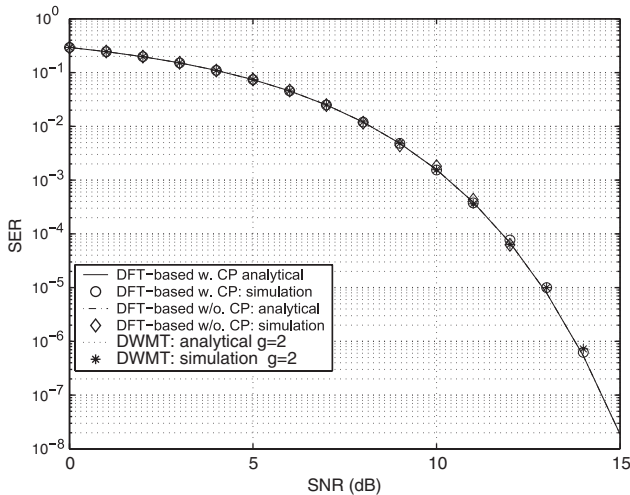


Fig. 5 Comparison of analytical and simulated performance of QPSK-MCM systems over AWGN channels ($P=32$)

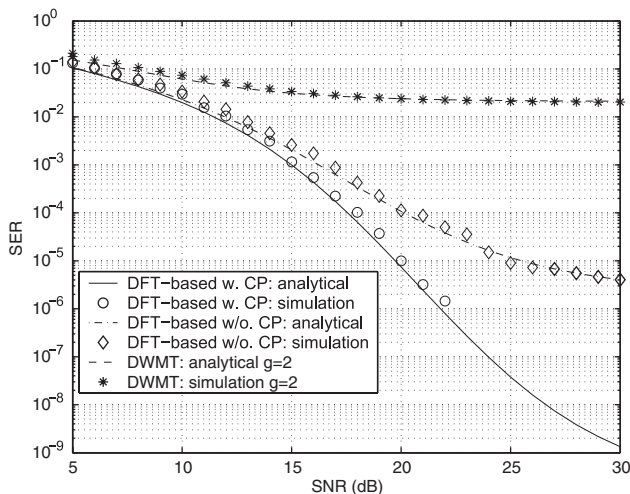


Fig. 6 Comparison of analytical and simulated performance of QPSK-MCM systems over channel $c_1(n)$ ($P=32$)

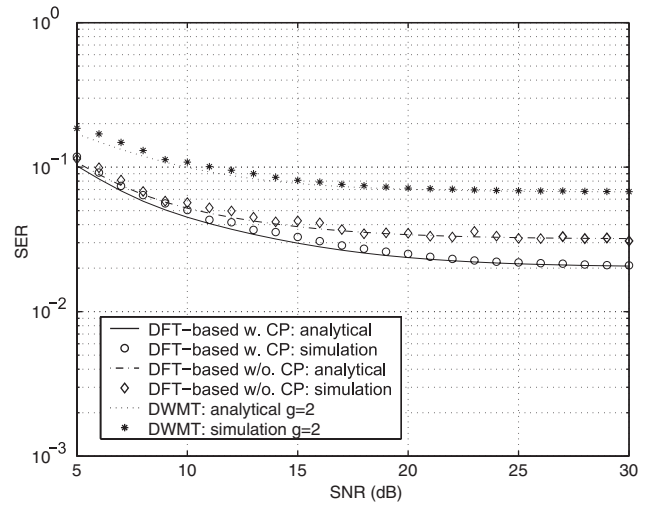


Fig. 7 Comparison of analytical and simulated performance of QPSK-MCM systems over channel $c_2(n)$ ($P=32$)

ISI is the dominant effect on the SER rather than ICI, which DWMT is designed to minimise. Moreover, as the filters in DWMT are of longer length, the dispersive channel may distort more symbols and increase ISI.

To investigate the error performance of the new MCM based on filter banks designed in Section 3, simulations are performed with a DFT-based OFDM, with zero-padded CP, a conventional DWMT system, of which the prototype filter is defined in (31), and the new MCM system based on complex-valued unitary filter banks. The filters of both the DWMT system and the new MCM system are of length $L = 2P$. As shown in Fig. 8, the new MCM system based on proposed complex-valued unitary filter banks has better SER than the DWMT system. Its performance is comparable to that of the DFT-based OFDM with CP. Note that, compared to the new MCM system, the transmission efficiency of the DFT-based OFDM with CP is decreased by a factor of $P/(P + L_k)$, where L_k is the length of CP and is chosen to be no less than the length of the channel.

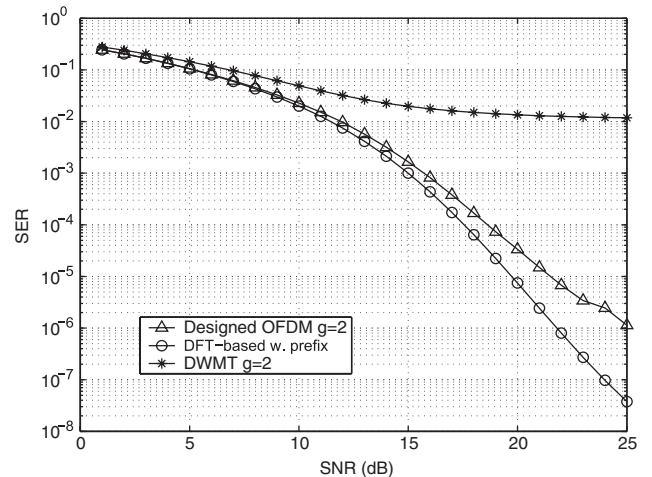


Fig. 8 System performance of different QPSK-MCM systems over channel $c_1(n)$ ($P=32$)

5 Conclusions

In this paper, we have presented a design method for a novel MCM system based on complex-valued multiband unitary filter banks to minimise the SER. To this end, a new

closed-form formula of the SER is derived for a generic MCM system with MPSK.

The presented complex-valued MCM system provides flexible frequency response design for different applications, by optimising filter banks towards different objective functions. It is especially useful when the frequency-selective channel characteristics are stationary or known a priori, which is often the case in wireline MCM systems such as in DSL applications.

Simulation results demonstrate that the designed MCM system outperforms the conventional DWMT systems in terms of the SER. The performance of the designed MCM is also comparable to that of the DFT-based OFDM with zero-padded CP, while the latter system compromises transmission efficiency for better error performance. Simulation results also show the consistency of numerical simulations and theoretical SER analysis using the new SER formula.

6 References

- 1 Sandberg, S.D., and Tzannes, M.A.: 'Overlapped discrete multitone modulation for high speed copper wire communications', *IEEE J. Sel. Areas Commun.*, 1995, **13**, (9), pp. 1571–1585
- 2 Akansu, A.N., and Lin, X.: 'A comparative performance evaluation of DMT(OFDM) and DWMT(DSBMT) based DSL communications systems for single and multitone inference'. IEEE Int. Conf. Acoustics Speech Signal Process. Proc. ICASSP, May 1998, Vol. 6, pp. 3269–3272
- 3 Mignone, V., and Morello, A.: 'CD3-OFDM: a novel demodulation scheme for fixed and mobile receivers', *IEEE Trans. Commun.*, 1996, **44**, (9), pp. 1144–1151
- 4 Liu, C.: 'The effect of nonlinearity on a QPSK-OFDM-QAM signal', *IEEE Trans. Consum. Electron.*, 1997, **43**, (3), pp. 443–447
- 5 Lei, S., and Lau, V.: 'Performance analysis of adaptive interleaving for OFDM systems', *IEEE Trans. Veh. Technol.*, 2002, **51**, (3), pp. 435–444
- 6 Weinstein, S.B., and Ebert, P.M.: 'Data transmission by frequency division multiplexing using the discrete Fourier transform', *IEEE Trans. Commun. Technol.*, 1971, **19**, pp. 628–634
- 7 Tzannes, M.A., Tzannes, M.C., and Resnikoff, H.L.: 'DMT systems, DWMT systems and digital filter banks'. IEEE Int. Conf. Commun. Proc., ICC, 1994, Vol. 1, pp. 311–315
- 8 Malvar, H.S.: 'Extended lapped transforms: properties, applications, and fast algorithms', *IEEE Trans. Signal Process.*, 1992, **40**, (11), pp. 2703–2714
- 9 Wong, K.M., Wu, J., Davidson, T.N., and Jin, Q.: 'Wavelet packet division multiplexing and wavelet packet design under timing error effects', *IEEE Trans. Signal Process.*, 1997, **45**, (12), pp. 2877–2890
- 10 Cherubini, G., Eleftheriou, E., Olcer, S., and Cioffi, J.M.: 'Filter bank modulation techniques for very high-speed digital subscriber lines', *IEEE Commun. Mag.*, 2000, **38**, (5), pp. 98–104
- 11 Akansu, A.N., Duhamel, P., Lin, X., and Courville, M.: 'Orthogonal transmultiplexers in communications: a review', *IEEE Trans. Signal Process.*, 1991, **46**, (4), pp. 979–995
- 12 Hwang, W., and Kim, K.: 'Performance analysis of OFDM on the shadowed multipath channels', *IEEE Trans. Consum. Electron.*, 1998, **44**, (4), pp. 1323–1328
- 13 Tjhung, T., Wang, X., and Ng, C.S.: 'Error performance evaluation of the MDPSK-DMT systems in AWGN and impulse noise', *IEEE Trans. Consum. Electron.*, 2000, **46**, (1), pp. 131–136
- 14 Pollet, T., Spruyt, P., and Moeneclaey, M.: 'The BER performance of OFDM systems using non-synchronized sampling'. IEE Int. Global Telecomm., Proc. IEEE GLOBECOM '94, Nov. 1994, pp. 253–257
- 15 Vandersteen, G., Verbeeck, J., Rolain, Y., and Schoukens, J.: 'Accurate bit-error-rate estimation for OFDM based telecommunication systems schemes in the presence of nonlinear distortions'. Proc. 17th IEEE Instrum. Meas. Technol. Conf., IMTC, 2000, Vol. 1, pp. 80–85
- 16 Lu, J., Tjhung, T., Adachi, F., and Huang, C.: 'BER performance of OFDM-MDPSK system in frequency-selective Rician fading with diversity reception', *IEEE Trans. Veh. Technol.*, 2000, **49**, (4), pp. 1216–1225
- 17 Chang, M.X., and Su, Y.T.: 'Performance analysis of equalized OFDM systems in Rayleigh fading', *IEEE Trans. Wirel. Commun.*, 2002, **1**, (4), pp. 721–732
- 18 Vaidyanathan, P.P.: 'Multirate systems and filter banks' (Prentice Hall, Englewood Cliffs, NJ, 1993)
- 19 Zhang, Q.T.: 'Error performance of noncoherent MFSK with L-diversity on correlated fading channels', *IEEE Trans. Wirel. Commun.*, 2002, **1**, (3), pp. 531–539
- 20 Zhang, Q.T., and Cui, X.W.: 'A closed-form expression for the symbol-error rate of M-ary DPSK in fast Rayleigh fading', *IEEE Trans. Commun.*, 2005, **53**, (7), pp. 1085–1087

- 21 Zhang, X.-P., Desai, M., and Peng, Y.-N.: 'Orthogonal complex filter banks and wavelets: some properties and design', *IEEE Trans. Signal Process.*, 1999, **47**, (4), pp. 1039–1048
- 22 Zou, H., and Tewfik, A.H.: 'Discrete orthogonal M-band wavelet decompositions'. IEE Int. Conf. Acoustics Speech Signal Process. Proc. ICASSP, 1992, Vol. 4, pp. IV605–608
- 23 Steffen, P., Heller, P.N., Gopinath, R.A., and Burrus, C.S.: 'Theory of regular M-band wavelet bases', *IEEE Trans. Signal Process.*, 1993, **41**, (12), pp. 3497–3511
- 24 Malvar, H.S.: 'Modulated QMF filter bank with perfect reconstruction', *Electron. Lett.*, 1990, **26**, (13), pp. 906–907
- 25 Rappaport, T.S.: 'Wireless communications: principles and practice' (Prentice Hall, 2002, 2nd edn.)
- 26 Stark, H., and Woods, J.W.: 'Probability, random processes, and estimation theory for engineers' (Prentice Hall, 1994)
- 27 Craig, W.: 'A new, simple, and exact result for calculating the probability of error for two-dimensional signal constellations'. Proc. IEEE Military Commun. Conf., MILCOM'91, October 1991, pp. 571–575
- 28 Simon, M.K., and Divsalar, D.: 'Some new twists to problems involving the Gaussian probability integral', *IEEE Trans. Commun.*, 1998, **46**, pp. 200–210
- 29 Weinstein, F.S.: 'Simplified relationships for the probability distribution of the phase of a sine wave in narrow-band normal noise', *IEEE Trans. Inf. Theory*, 1974, **20**, pp. 658–661
- 30 Pawula, R.F., Rice, S.O., and Roberts, J.H.: 'Distribution of the phase angle between two vectors perturbed by Gaussian noise', *IEEE Trans. Commun.*, 1982, **30**, pp. 1828–1841
- 31 Jeffreys, H., and Jeffreys, B.S.: 'Methods of mathematical Physics' (Cambridge University Press, Cambridge, England, 1988, 3rd edn.)

7 Appendix

7.1 Derivation of formulation 1

As shown in Fig. 2, the data sequence to be transmitted over channel, $s(n)$, is the sum of output signals of all modulation filters, i.e.

$$s(n) = \sum_{p=0}^{P-1} \sum_{i=-\infty}^{\infty} x_p(i) f_p(n - iK) \quad (32)$$

At the receiving end, the received signal $r(n)$ is distorted by channel noise and interferences due to the nonideal channel. It can be expressed as

$$\begin{aligned} r(n) &= s(n) * c(n) + e(n) \\ &= \sum_{k=-\infty}^{\infty} s(k) c(n - k) + e(n) \end{aligned} \quad (33)$$

where '*' represents convolution. As indicated in Fig. 2, $r(n)$ is passed to the filter-bank demodulator h_p , $p = 0, 1, \dots, P - 1$, and the output of each subchannel demodulation filter is downsampled by factor K . The received symbol for the subchannel p_1 at time frame n_1 can be expressed as

$$y_{p_1}(n_1 + d) = \sum_{m=-\infty}^{\infty} r(m) h_{p_1}(n_1 K - m) \quad (34)$$

By substituting (32) and (33) into (34),

$$\begin{aligned} y_{p_1}(n_1 + d) &= \sum_{p=0}^{P-1} \sum_{n=-\infty}^{\infty} x_p(n) \sum_{m=-\infty}^{\infty} \sum_{k=-\infty}^{\infty} f_p(k - nK) \\ &\quad \times c(m - k) h_{p_1}(n_1 K - m) + \sum_{m=-\infty}^{\infty} e(m) h_{p_1}(n_1 K - m) \end{aligned} \quad (35)$$

Let $j = m - k$ and $l = k - nK$, (35) becomes

$$\begin{aligned} y_{p_1}(n_1 + d) &= \sum_{p=0}^{P-1} \sum_{n=-\infty}^{\infty} x_p(n) \sum_{j=-\infty}^{\infty} c(j) f_p(l) h_{p_1} \\ &\quad \times ((n_1 - n)K - j - l) + \zeta \end{aligned} \quad (36)$$

where ζ is defined in (11). By defining $\alpha_{pp_1}(n)$ and ζ as in (13) and (12), respectively, (36) can be reduced to (9).

7.2 Proof of Theorem 1

The idea is to find out the probability density function (PDF) of $y_{p_1}(n_1 + d)$ and then calculate the probability of error for optimal phase detector of each subchannel.

In the MPSK modulation scheme, the transmitted symbol $x_p(n)$ is coded as

$$x_p(n) = \sqrt{\epsilon_x} e^{j\theta_k}, k = 0, 1, \dots, M-1 \quad (37)$$

where the transmitted phase $\theta_k = \{(2\pi k)/M\}$. We have $E[x_p(n)] = 0$ and $\text{Var}[x_p(n)] = \epsilon_x$, for $p = 0, 1, \dots, P-1$.

Owing to the fact that coefficients of modulator/demodulator and channels can be complex-valued, $y_{p_1}(n_1 + d)$ may be complex-valued as well. We denote the real and imaginary parts of $y_{p_1}(n_1 + d)$ as a and b .

To obtain the expression for the SER of $y_{p_1}(n_1 + d)$, the joint probability density function $f_{AB}(a, b)$ must be formulated. In the following, we first derive the characteristic function of $y_{p_1}(n_1 + d)$.

As $e(n)$ is a zero-mean Gaussian process, it is easy to see from (11) that ξ is a Gaussian process with zero mean and variance $\sigma_\xi^2 = \sigma_n^2$.

Generally, the transmitted source signal samples at different time instant n are independent and identically distributed. It can then be inferred that symbol $x_p(n)$ at different time instant n and different channel p are independent and identically distributed. From (12), the interference ζ is the weighted sum of independent identically distributed (iid) random variables, $x_p(n)$, and each with mean μ_x and variance σ_x^2 . Using the same argument as in [25] and other references therein, as the quantity of $x_p(n)$ becomes large, ζ approaches a Gaussian random process according to the central limit theorem (CLT) [26]. Moreover, the mean and variance of ζ can be calculated as

$$\mu_\zeta = \sum_{p, p \neq p_1} \sum_n \alpha_{pp_1}(n) E[x_p(n)] + \sum_{n, n \neq n_1} \alpha_{p_1 p_1}(n) E[x_{p_1}(n)] = 0 \quad (38)$$

$$\begin{aligned} \sigma_\zeta^2 &= \sum_{p, p \neq p_1} \sum_n |\alpha_{pp_1}(n)|^2 \text{Var}[x_p(n)] \\ &\quad + \sum_{n, n \neq n_1} |\alpha_{p_1 p_1}(n)|^2 \text{Var}[x_{p_1}(n)] \\ &= \left[\sum_{p, p \neq p_1} \sum_n |\alpha_{pp_1}(n)|^2 + \sum_{n, n \neq n_1} |\alpha_{p_1 p_1}(n)|^2 \right] \epsilon_x \end{aligned} \quad (39)$$

Note that this Gaussian assumption of the interference ζ by the CLT is commonly used in multichannel/multiuser communication systems [25]. It makes the analysis tractable and is a realistic assumption proved by simulations.

As the noise ξ and the interference ζ are Gaussian processes and independent of each other, the received symbol $y_{p_1}(n_1 + d)$ is a Gaussian random variable with mean \bar{y}_{p_1} and variance

$$\begin{aligned} \sigma_y^2 &= \sigma_\xi^2 + \sigma_\zeta^2 \\ &= \sigma_n^2 + \left[\sum_{p, p \neq p_1} \sum_n |\alpha_{pp_1}(n)|^2 + \sum_{n, n \neq n_1} |\alpha_{p_1 p_1}(n)|^2 \right] \epsilon_x \end{aligned} \quad (40)$$

Hence, the characteristic function of $y_{p_1}(n_1 + d)$ can be expressed as

$$\Phi_y(v) = \exp\left(j\bar{y}_{p_1}v - \frac{v^2\sigma_y^2}{2}\right) \quad (41)$$

The joint PDF of a and b can then be obtained with the characteristic function of $y_{p_1}(n_1 + d)$ as

$$f_{AB}(a, b) = \frac{1}{2\pi\sigma_y^2} \exp\left(-\frac{[a - \text{Re}(\bar{y}_{p_1})]^2 + [b - \text{Im}(\bar{y}_{p_1})]^2}{2\sigma_y^2}\right) \quad (42)$$

where $\text{Re}(\cdot)$ and $\text{Im}(\cdot)$ represent the real and imaginary parts of a complex value, respectively.

With the change of variables from (a, b) to (V, Θ_y) , where $V = \sqrt{a^2 + b^2}$ and $\Theta_y = \tan^{-1}(b/a)$, the PDF of the detected phase Θ_y can be obtained by

$$\begin{aligned} f_{v\Theta}(V, \Theta_y) &= \frac{V}{2\pi\sigma_y^2} \\ &\times \exp\left(-\frac{V^2 + |\bar{y}_{p_1}|^2 - 2V|\bar{y}_{p_1}|\cos(\Theta_y - \theta_{\bar{y}_{p_1}})}{2\sigma_y^2}\right) \end{aligned} \quad (43)$$

where $\theta_{\bar{y}_{p_1}} = \tan^{-1}(\text{Im}(\bar{y}_{p_1})/\text{Re}(\bar{y}_{p_1}))$ is the phase of the output constellation point \bar{y}_{p_1} .

As $y_{p_1}(n_1 + d)$ is a Gaussian process, the optimal phase detector based on the maximum likelihood (ML) detection criterion can be employed to perform detection for subchannel p_1 . The operation principle of the optimal phase detector is to compute the phase of $y_{p_1}(n_1 + d)$ and select the constellation point, from the constellation set of \bar{y}_{p_1} , with the smallest phase difference relative to $y_{p_1}(n_1 + d)$. Then, the transmitted symbol can be determined due to the one-to-one mapping relation between the constellation points of $x_{p_1}(n_1)$ and \bar{y}_{p_1} . The decision boundary for $y_{p_1}(n_1 + d)$ can be determined based on the constellation points of \bar{y}_{p_1} . According to (10), \bar{y}_{p_1} is a scaled version of $x_{p_1}(n_1)$ and the weight $\alpha_{p_1}(n_1)$ is a constant for a given subchannel, i.e. the phase difference between the constellation points of \bar{y}_{p_1} is the same as that of transmitted symbol $x_{p_1}(n_1)$. Hence, the phase difference of any two adjacent constellation points of \bar{y}_{p_1} is $2\pi/M$. Without loss of generality, we assume the phase of transmitted symbol $x_{p_1}(n_1)$ is 0. In this case, no decision error will happen if the phase of $y_{p_1}(n_1 + d)$ falls inside the range Λ , which is calculated as

$$\Lambda = \left[-\frac{\pi}{M} + \theta_{\bar{y}_{p_1}}, \frac{\pi}{M} + \theta_{\bar{y}_{p_1}}\right] \quad (44)$$

To calculate the SER, the integration range of the variable V in (43) is $[0, +\infty)$, which is computationally complex. Similar to the methods in [27–30], we convert the integration over the infinite range into an integration over a finite range by changing variables (V, Θ_y) in (43) to (r, ψ_y) , as shown in Fig. 9. Note that, y is the received symbol, Θ_y and V are phase and radius of y , respectively. The constellation point corresponding to the transmitted symbol, with phase zero, is denoted as \bar{y}_{p_1} . The received symbol point y , at a distance r from \bar{y}_{p_1} and ψ_y , is the angle between vectors $\vec{\bar{y}_{p_1}y}$ and $\vec{o\bar{y}_{p_1}}$.

The following expressions can be derived from Fig. 9,

$$V \cos(\Theta_y - \theta_{\bar{y}_{p_1}}) - |\bar{y}_{p_1}| = r \cos(\psi_y) \quad (45)$$

$$r \sin(\psi_y) = V \sin(\Theta_y - \theta_{\bar{y}_{p_1}}) \quad (46)$$

therefore

$$V = \sqrt{r^2 + 2|\bar{y}_{p_1}|r \cos(\psi_y) + |\bar{y}_{p_1}|^2} \quad (47)$$

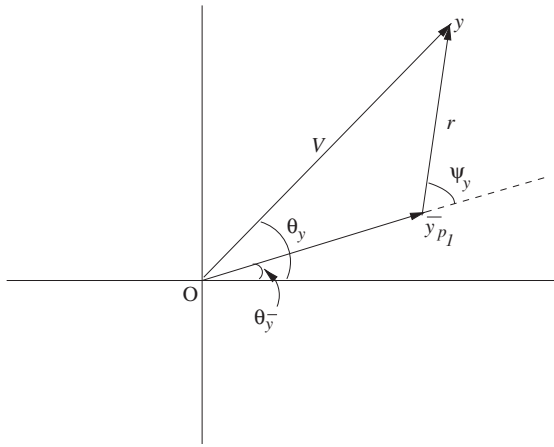


Fig. 9 Illustration of change of variables

$$\Theta_y = \tan^{-1} \left(\frac{r \sin(\psi_y)}{r \cos(\psi_y) + |\bar{y}_{p1}|} \right) + \theta_{\bar{y}_{p1}} \quad (48)$$

or alternatively

$$r = \sqrt{V^2 - 2V \cos(\Theta_y - \theta_{\bar{y}_{p1}}) |\bar{y}_{p1}| + |\bar{y}_{p1}|^2} \quad (49)$$

$$\psi_y = \tan^{-1} \left(\frac{V \sin(\Theta_y - \theta_{\bar{y}_{p1}})}{V \cos(\Theta_y - \theta_{\bar{y}_{p1}}) - |\bar{y}_{p1}|} \right) \quad (50)$$

According to the change of variable theorem [31],

$$f_{r\psi_y}(r, \psi_y) = f_{V\Theta}(V, \Theta_y) \left| \frac{\partial(V, \Theta_y)}{\partial(r, \psi_y)} \right| \quad (51)$$

where $|\partial(V, \Theta_y)/\partial(r, \psi_y)|$ is the determinant of Jacobian matrix $[\partial(V, \Theta_y)/\partial(r, \psi_y)]$. Substituting (47) and (48) into (51), the PDF of (r, ψ_y) is obtained:

$$f_{r\psi_y}(r, \psi_y) = \frac{r}{2\pi\sigma_y^2} \exp\left(-\frac{r^2}{2\sigma_y^2}\right) \quad (52)$$

The SER can then be calculated as

$$P_{e,p1} = 2 \int_0^{\frac{(M-1)\pi}{M}} d\psi \int_R^\infty f_{r\psi_y}(r, \psi_y) dr \quad (53)$$

where $R = |\bar{y}_{p1}| \sin(\pi/M) / \sin(\psi_y + \pi/M)$, and the expression of the SER can be simplified as in (14), where

$$\gamma = \frac{|\bar{y}_{p1}|^2}{\sigma_y^2} \quad (54)$$

By substituting (10) and (40) into (54), we obtain (15). Thus, Theorem 1 is proven.